International Journal of Biological Macromolecules 248 (2023) 125980

Contents lists available at ScienceDirect

International Journal of Biological Macromolecules

journal homepage: www.elsevier.com/locate/ijbiomac

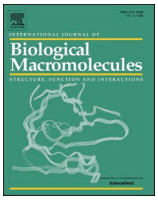

Nanofiber mats functionalized with *Mentha piperita* essential oil stabilized in a chitosan-based emulsion designed via an electrospinning technique

Javier Lamarra [a,b,*], Sandra Rivero [a,b], Adriana Pinotti [a,d], Daniel Lopez [c]

[a] Centro de Investigación y Desarrollo en Criotecnología de Alimentos (CCT-CONICET La Plata, CIC, UNLP), 47 y 116 S/N, La Plata, Buenos Aires, Argentina
[b] Facultad de Ciencias Exactas, UNLP, La Plata 1900, Argentina
[c] Instituto de Ciencia y Tecnología de Polímeros, ICTP-CSIC, Calle Juan de La Cierva 3, 28006 Madrid, Spain
[d] Facultad de Ingeniería, UNLP, La Plata 1900, Argentina

ARTICLE INFO

Keywords:
Electrospinning
Rotating drum collector
Polyvinyl alcohol
Chitosan emulsion
Peppermint essential oil
Mentha piperita essential oil

ABSTRACT

A nanostructured device based on poly(vinyl alcohol) (PVA) loaded with a cross-linked chitosan (CH) emulsion, soy lecithin, and peppermint essential oil (*Mentha piperita*) was designed for topical applications using an electrospinning instrument coupled to a rotary drum collector. Different suspensions were obtained by varying the PVA to emulsion ratio (PVA:Em) 87.5:12.5, 82:18, and 75:25, using a PVA solution as a control. ATR-FTIR spectra confirmed the interactions among the components of the system. Scanning electron microscopy (SEM) of the mats evinced that the aligned fiber diameter decreased with higher proportions of emulsion while dynamic mechanical analysis (DMA) revealed a decrease in the storage modulus.

The entrapment of the functionalized emulsions not only improved the elongation of the matrices but also provided them with greater structural integrity compared to the single PVA matrix. The most favorable formulation in terms of mechanical properties was found to be the 82:18 ratio.

After 1 h of close contact between the 82:18 matrix and a porcine skin explant, the latter was examined by confocal microscopy, which revealed the localization of the essential oil mainly on the surface of the stratum corneum (SC).However, after 7 h of contact, the distribution of the peppermint EO throughout the viable epidermis was observed, which was further supported by ATR-FTIR studies.

Tailored electrospun matrices would have potential applications as devices for topical or transdermal treatments due to their vehiculization role that allows the diffusion of peppermint essential oil as a skin penetration enhancer.

1. Introduction

Within the field of nanotechnology, the design of nanostructures has been extensively explored. Specifically, the electrospinning technique is one of the most versatile methods to obtain nanofibers facilitating the nanoencapsulation of active compounds [1–3].

The nanofibers obtained by electrospinning technique have a high loading capacity of active compounds and a high surface area to volume ratio and large number of inter/intra fibrous pores resulting in a material with low density [4]. On the other hand, the electrospun nanofibers present important advantage from biomedical point of view due the fiber can mimic the extracellular matrix [5].

There are reports in literature focusing on the generation of hybrid nanofibrous scaffolds for tissue engineering, wound dressing, drug delivery systems and enzyme immobilization, among the most relevant applications [6]. Given the versatility of fibrous nanostructures as carrier materials, the role of electrospun nanofibers as a controlled and sustained delivery system of an active compound has been extensively studied and has demonstrated enhanced therapeutic efficacy and reduced toxicity [7].

The assembly of an active compound by the electrospinning technique can be helpful in the fabrication of different hierarchical structures. This can be done by various strategies, such as adding the active compound to the polymer nanofiber as nanoparticles, formulating a composite system, or encapsulating the drug in the electrospun nanofibers [7].

* Corresponding author at: Centro de Investigación y Desarrollo en Criotecnología de Alimentos (CCT-CONICET La Plata, CIC, UNLP), 47 y 116 S/N, La Plata, Buenos Aires, Argentina.
E-mail address: jlamarra11@gmail.com (J. Lamarra).

https://doi.org/10.1016/j.ijbiomac.2023.125980
Received 29 May 2023; Received in revised form 15 July 2023; Accepted 23 July 2023
Available online 26 July 2023

In this technique, the voltage application produces a Taylor cone generating a jet with the consequent solvent evaporation. Upon reaching a collector, a thin film is produced conformed by micro and nanofibers [8].

The polymeric solution flows through a needle connected to a voltage source that simultaneously is connected to a collector [9]. The collector is another crucial component in electrospinning (*E*-spin). Various types of collectors are available, such as drum collectors, plate collectors, parallel plate collectors, cocoon collectors, and disc collectors, among others. The selection of an appropriate collector primarily depends on the intended application of the fabricated nanofibers. In laboratory-level experiments, drum collectors are commonly employed to obtain well-aligned and nanosized fibers.

The configuration of the rotating drum allows for controlled and organized fiber deposition, contributing to the production of desired nanofiber characteristics giving like results aligned nanofibers but without obtaining thick mats [9,10].

There are two geometries for the collector used in the electrospinning technique, a metallic plate, or a rotating metallic collector. The conventional flat plane collectors produce nanofibers with randomly oriented distribution, while rotating rods and rotating drums can be used as a ground platform to collect aligned fibers [9].

The ability to control fiber alignment is greatly sought after to produce anisotropic mats due to the broad range of properties and biological effects that can be achieved in various fields, including tissue engineering [11], cell growth [12], drug delivery [13], and other biomaterial applications [14].

Several variables play a role when the electrospinning process is carried out, such as modification of intrinsic parameters of the polymer solution (average molecular weight, viscosity, surface tension, and conductivity of the solution) [1–3].

One of the environmentally friendly polymers used in the development of functionalized nanofibers is the poly(vinyl alcohol) (PVA). It is a non-toxic, biocompatible, hydrophilic synthetic polymer with good chemical, thermal, and mechanical stability which has found extensive applications in the preparation of various biomaterials, including films, membranes, hydrogels, scaffolds, and nanofibers [15,16]. PVA contains residual vinyl acetate groups that give it an amphiphilic character, demonstrating its ability as a surfactant agent [17].

In the pharmaceutical field, PVA is used in topical and ophthalmic formulations, serving as a stabilizing agent for emulsions and enabling sustained release formulations for oral use. In addition, PVA has proved to be an ideal material for the production of electrospun nanofibers loaded with active ingredients [18].

Diverse active compounds such as antiparasitic compounds [19], antioxidants [15], antibiotics [16], and essential oils [1] can be supported in an electrospun matrix. Applications of essential oils (EO) are an emergent area of research and innovation to develop active materials [20].

Essential oils have been used in the production of cosmetics and pharmaceuticals mainly due to their antioxidant and antimicrobial properties [21]. Because of their high content of terpenes, EOs are used as penetration enhancers of the active agents through the skin.

Peppermint essential oil (*Mentha piperita*) consists mainly of menthol and menthone along with several other minor constituents, including menthofuran, 1,8-cineole, and limonene. The active compound has been used as an anti-inflammatory, analgesic, antifungal, and antimicrobial agent [22]. It also has been applied for wound dressing, food preservation, and pharmaceuticals [23,24].

Two main methods have been developed as strategies to protect EOs: direct encapsulation of the essential oil through fiber formation by electrospinning [25,26] or entrapment of the essential oil after the formation of the fibers [27]. While the direct incorporation of essential oils (EO) into a hydrophobic matrix may seem straightforward and eliminates the need for additional synthesis steps, it has some drawbacks. One of these drawbacks is the requirement of organic solvents such as dimethylformamide (DFM) and chloroform, which can release toxic vapors that can be harmful to human health [28]. A more effective approach is the use of hydrophilic emulsions, which allow the encapsulation of essential oils within a hydrophilic matrix [1,29]. This alternative approach provides advantages in terms of safety and enables the controlled release of the essential oil.

Soy lecithin has the role of acting as a stabilizer by rapidly adsorbing on the droplet surface, reducing the O/W interfacial tension between the oil and water phases, and imparting a negative surface charge, resulting in high repulsive force interactions against the destabilization processes [30]. One of the most common strategies to produce a stable emulsion is to combine it with stabilizers as chitosan [31].

Chitosan (CH) is a cationic polyelectrolyte that can be assembled to form a layer or interfacial film on the oil drop promoting better system stability [1,32]. It is a biodegradable and biocompatible polymer, which contains amino groups in its structure [33]. These amino groups can be protonated at acidic pHs, which confers to this polymer the highest reactivity, allowing its use as an encapsulation agent [5,34].

Regarding the use of chitosan as a biopolymer for the encapsulation of essential oils, different authors have reported the encapsulation capacity of *Valeriana officinalis* essential oil [35] and *Thymus vulgaris* essential oil [36], among others. In previous work, the synthesis of a crosslinked emulsion based on chitosan and PVA to encapsulate cabreuva essential oil was reported by Lamarra et al. [1]. The positive charge of chitosan allows the preparation of nanoparticles by interaction with anions, such as sodium citrate, faciliting the entrapment of the hidrophobic essential oil in a hydrophilic film.

To the best of our knowledge, there is hardly any study about the development and characterization of eco-friendly aligned electrospun mats of PVA with *Mentha piperita* essential oil stabilized in a crosslinked chitosan-based emulsion and their application as a functionalized wound dressing. Considering that chemical components of essential oils have high volatility, low water solubility, and are susceptible to degradation from temperature, light, oxygen, and moisture, this research was focused on the encapsulation of the essential oil-based emulsions within nanostructures formed using chitosan, poly(vinyl alcohol), and soy lecithin, studying the size particle and the zeta potential. Once the appropriate crosslinked emulsion was selected, matrices consisting of oriented nanofibers were formed using the electrospinning technique, with poly(vinyl alcohol) serving as the supporting material in various proportions. An in-depth study of the entrapment of the encapsulated emulsions on the morphological, structural, and thermomechanical properties of nanostructures obtained by electrospinning was also examined. Furthermore, the diffusion of the EO from the electrospun mat upon contact with a porcine skin explant was analyzed by confocal microscopy taking advantage of the *Mentha piperita* fluorescence, and its penetration into the *stratum corneum* was confirmed by ATR-FTIR studies.

2. Materials and methods

2.1. Materials

Chitosan (CH) with 85 % of deacetylation degree and Mw = 3.2×10^5 Da was supplied by PolymarCiencia and Nutricao (Fortaleza, Brazil) while poly(vinyl alcohol) (PVA) with a hydrolysis degree of 86–89 % and molecular mass range between 50 and 55 kDa was acquired from Dupont (USA). Soybean lecithin was purchased from Parafarm (Argentina), sodium citrate was supplied by Cicarelli (Argentina), and *Mentha piperita* essential oil was acquired from Esencias del Bosque (La Plata, Argentina).

2.2. Methods

2.2.1. Formulation and characterization of O/W encapsulated emulsions

In the first step of the experimental procedure, a similar method

proposed by Lamarra et al. [1] was followed to formulate an oil-in-water emulsion (O/W). The emulsion was prepared using two polymers, polyvinyl alcohol (PVA) and chitosan (CH) which were mixed in a 1:1 ratio (v/v).

To prepare the chitosan solution, the biopolymer was dissolved in a 0.75 % (w/v) acetic acid solution 0.75 % (v/v)for 12 h. On the other hand, the PVA used as a stabilizing agent for the emulsion was solubilized in water at 90 °C for 16 h to obtain a 0.75 % (w/v) solution.

To form the emulsions, different quantities of soybean lecithin (1 %, 5 %, and 10 % w/w) were added to the composite solution of PVA and CH. Lecithin is a zwitterionic phospholipid that reduces the surface tension between two phases. The soybean lecithin used, defatted and enriched in phosphatidylcholine, has the role of acting as a stabilizer. This resulted in three different emulsion formulations: Em_1, Em_5, and Em_{10}, where the subscript indicates the lecithin concentrations relative to the total emulsion weight.

After the addition of the peppermint essential oil at a concentration of 7.5 % (v/v), the system was subjected to homogenization using an Ultraturrax T-25 to form the emulsion (Janke and Kunkel, IKALabortechnik, Germany) operating at 21,000 rpm for 10 min to achieve a uniform distribution of the essential oil within the emulsion. To further reduce droplet size and enhance system stability, the emulsion was subjected to an ultrasound treatment using Sonics VCX-750 ultrasonic processors (Vibra Cell, USA) for 10 min at 20 % amplitude.

In the second step of the process, the emulsions were crosslinked using sodium citrate at a concentration of 0.125 % (*w/v*). The crosslinking was performed through the ionic gelation technique, which involves the formation of a gel network through the interaction between the polymer and the crosslinking agent.

The zeta potential (ZP) and hydrodynamic diameter (D_H) of the active crosslinked emulsions were found to be simple techniques that could be used to study the surface charge of NPs and their hydrodynamic size, respectively. These determinations were performed using a Malvern Zeta Sizer Nanozs (Malvern Instruments Ltd., UK).

Size measurements were performed by dynamic light scattering (DLS) using a 4 mW He—Ne laser at a wavelength of 633 nm and a detection angle of 173°. The size distribution profiles were obtained by analyzing the correlation function in the instrument software. In this sense, the intensity of the scattered light was used to calculate the mean hydrodynamic diameter (*Z*-average mean). For each sample, the data average was calculated from a minimum of five measurements.

2.2.2. Preparation of fiber-forming suspensions

Film-fiber suspensions to be submitted to the electrospinning process were obtained mixing PVA 16 % and O/W Em_{10} emulsion (described in 2.2.1) for 24 h. To obtain the composite suspensions, the PVA solution to emulsion ratio were 87.5:–12.5, 82:18, and 75:25 (Supplementary material Table S1). A solution of PVA prepared at 16 % (w/v) was used as a control (PVA).

2.2.3. Rheological characterization of fiber-forming suspensions

To study the rheological behavior of polymeric solutions, flow experiments were carried out in a TA instrument controlled stress rheometer ARG2 (New Castle, Delaware, USA). The determinations were conducted on fiber-forming suspensions at 25 °C using the parallel plate of rough surfaces with a gap between the plates of 1 mm, evaluating the apparent viscosity at 500 s^{-1}.

2.2.4. Preparation of fibrous matrices by electrospinning

The formation of fibers was carried out by using homemade equipment (Supplementary material, Fig. S1), with a voltage source operating at 18 kV, an injection pump at a constant flow rate of 0.4 ml/min [1], and a distance from the needle tip to the collector of 10 cm. The used collector was a rotating drum working at an angular velocity of 1300 rpm. The average time of the electrospinning process was 16 h.

2.2.5. Scanning electron microscopy (SEM)

A FEI Quanta 200 electronic microscope (SEM) operated with an acceleration voltage of 15 kV was used to analyze the morphology and diameter of the fibers. The fiber diameter distribution was measured using the Fiji program (Image J, NIH, USA).age J, NIH, USA).

2.2.6. Contact angle

The contact angle was determined with an EasyDrop Standard Goniometer model FM140 (KRÜSS GmbH, Hamburg, Germany) equipped with a camera. To determine the water contact angle, the Drop Shape Analysis SW21 (DSA1) software was used. A minimum of 6 replicates of each sample were analyzed.

2.2.7. Thermal analysis

The study of thermal behavior was conducted by two techniques: differential scanning calorimetry (DSC) and thermogravimetric analysis (TGA). By using a DSC Q2000 (TA Instruments, USA), different endothermic and exothermic signals were recorded by the application of a heating scan from -50 °C to 250 °C at a speed scan of 10 °C min^{-1} under an inert atmosphere of N_2. On the other hand, the TGA analysis allowed evaluation of the weight loss by using equipment TA Q500 (TA Instruments, USA). The samples were determined between 30 and 600 °C under an inert atmosphere (N_2) with a scan of 10 °C min^{-1}.The thermal behavior study was performed using two techniques: differential scanning calorimetry (DSC) and thermogravimetric analysis (TGA). Using a DSC Q2000 (TA Instruments, USA), various endothermic and exothermic signals were recorded by applying a heating scan from -50 °C to 250 °C at a scan speed of 10 °C min^{-1} under an inert N_2 atmosphere. On the other hand, the TGA analysis allowed the weight loss to be evaluated using the TA Q500 device (TA Instruments, USA). The samples were determined between 30 °C and 600 °C under an inert atmosphere (N_2) with a scan of 10 °C min^{-1}.

2.2.8. Mechanical properties

The mechanical properties of the electrospun mats were evaluated by tension tests in a Qtest 1/L Elite equipment by using a 100 N load cell at room temperature. The initial length was 10 mm and the elongation rate was settled at 10 mm min^{-1}. To carry out the assays, rectangle specimens of 10 mm in length and 5 mm in width were cut from the matrix. Strain and stress were calculated.

2.2.9. Dynamic mechanical analysis (DMA)

Dynamic mechanical spectra of the matrices were obtained with DMTA Mettler DMA 861e using tension clamps, which allow the analysis of the relaxations of the material, working at 1, 3, 10, and 30 Hz with an amplitude of the applied force of 15 μm.

2.2.10. ATR-FTIR

The electrospun matrices functionalized with *Mentha piperita* essential oils were analyzed by using Fourier transforms infrared spectroscopy equipment in the attenuated total reflectance mode by using a spectrometer ATR- FTIR (Nicolet, iS10, ThermoScientific, Madison, USA). The data were recorded in the range 4000–400 cm^{-1} with a resolution of 4 cm^{-1}.

2.2.11. Diffusion of peppermint EO by CLSM and ATR-FTIR

The diffusion of peppermint essential oil was determined using 24 mm diameter disks of ear porcine skin (provided by a butcher shop) following a similar procedure to that described by Izquierdo et al. [37]. The surface of the specimen was cleaned and stored in polyethylene bags at −20 °C until use. A Saärbruken device, which operates under non-occlusive conditions, was used for the ex-vivo assay [38,39]. A filter disk embedded in PBS buffer was placed at the bottom of the cavity of the dispositive on which a porcine skin explant was located. A specific weight (10 g) was used to ensure optimal and close contact between the explant and the nanofiber matrix.

The diffusion tests were carried out in an ambient atmosphere of 100 % and a temperature of 37 °C. Essential oil diffusion was evaluated at two different times, 1 and 7 h. The selected sample to carry out the tests was 82:18 due to its optimal mechanical properties and the significant proportion of active emulsion in relation to the PVA matrix. To assess the diffusion of the active compound through the skin, explant slices previously frozen at −80 °C, were cut into 20 μm histological sections by using a Thermo-Shandon-Cryotome (FSE) Microtome. The observation was carried out by confocal laser microscopy (Olympus FV-1000) with a DAPI filter. On the other skin specimen sample, incubated with a functionalized film, optical sectioning was performed, taking images in the *Z*-axis every 10 μm. The intensity of the DAPI-specific fluorescence signals was analyzed using the Fiji-Image J software.

Complementary studies through ATR-FTIR spectroscopy were carried out on the porcine skin explants subjected to diffusion tests, analyzing the spectral region between 3000 and 2800 cm^{-1} to evaluate the penetration of the essential oil or the active emulsion, either as compounds assembled on an electrospun matrix after close contact with the skin explant.

2.2.12. Statistical analysis

Statistical analysis was performed by using the InfoStat Software (Version 2008) (InfoStat Group, Argentina). Analysis of variance (ANOVA), linear regressions, and Fisher LSD mean comparison test were applied. The significance level used was 0.05.

3. Results and discussion

3.1. Emulsion characterization

The functionalized emulsions were characterized through hydrodynamic diameter (D_H) and zeta potential (ZP) studies.

As can be seen in Table 1, all formulations presented a positive ZP value, characteristic of suspensions formed from a polycationic compound such as chitosan [40]. The decrease in the ZP values was correlated with the lecithin concentration, which could be attributed to the negative charges of phosphate groups in the structure of the surfactant agent [41]. Regarding the ZP values, the formulated emulsions could be considered stable in terms of colloidal interactions that prevent coalescence, since they showed values greater than +30 mV [40]. The hydrodynamic diameter (D_H) of all formulations presented a relatively low value of the polydispersity index, which is a good indicator of the dispersion degree of the drops. On the other hand, the formulation with the highest concentration of soy lecithin (Em_{10}, at 10% w/w) presented the lowest D_H value. Consequently, this was the formulation selected to assemble with the PVA matrix to obtain the electrospun nanofibers. The decrease in the drop size with increasing lecithin concentration might be due to the emulsifying properties of this compound which can induce both, hydrophilic and hydrophobic interactions with the essential oil [41]. Andrade et al. [42] explain that lecithin with the highest content of phosphatidylcholine produces liposomes with homogeneous membranes due to a large number of groups with hydrophilic heads, which promote the spontaneous formation of these vesicles.

Based on these results, the formulation with the best performance was chosen for the electrospinning process.

Table 1
Characterization of emulsions functionalized with *Mentha piperita* EO using zeta potential (ZP) and hydrodynamic diameter (D_H).

Emulsion	ZP (mV)	D_H (nm)	PDI
Em_1	52.3[b]	432.5[c]	0.218[c]
Em_5	52.5[b]	386.9[b]	0. 122[a]
Em_{10}	46.7[a]	354.2[a]	0.176[b]

[a] Different super index in the same column indicates significant differences among samples ($p < 0.05$).

3.2. Rheological behavior of polymeric solutions

By selecting the appropriate process parameters, it is possible to control the diameter and properties of the fibers. The concentration and viscosity of the polymer solution are key factors that have the most significant influence on the size and morphology of the fibers. In this sense, the viscosity of the solution determines the extent of the solution stretching. In addition, the blending of nonionic polymers with a cationic polymer as the chitosan helps the electrospinning process [43].

The flow curves of all film-forming emulsions showed non-Newtonian and shear thinning behavior with n values ranging from 0.82 to 0.88, which were fitted to the Ostwald-de Waele model.

$$\tau = k_v \dot{\gamma}^n \quad (1)$$

where, τ is the shear stress, γ is the shear rate, k_v is the consistency index, and n the flow behavior index. The apparent viscosity (η) was determined at 500 s^{-1}. The estimated rheological parameters are shown in Table S2 (Supplementary material).

The value of $n < 1$ indicated the required shear thinning behavior necessary for electrospinning. The interactions between the two phases led to the viscoelastic behavior of the suspensions and, consequently, to the formation of uniform fibers during electrospinning [44]. Furthermore, the apparent viscosity of the PVA solution which was 2.75 Pa.seg at 500 s^{-1} experienced a reduction with increasing emulsion entrapment (Table 2). As stated by Higashi et al. [45], the typical viscosity range for electrospinning is generally less than 5 Pa·s.

According to Pal et al. [42], it has been shown that the flow of an emulsion subjected to high voltage by electrospinning processing causes the dispersed droplets to show a tendency to move inward during the flow and form the core of the fiber, while the sheath is formed by the continuous phase would act as wall material.

The results obtained suggest that the entrapment of the emulsion at the tested concentrations, although it decreased the viscosity compared to PVA control, did not change the flow behavior within the range of the analyzed shear rates. Similar results were reported by Fonseca et al. [46] who observed a decrease in the apparent viscosity of potato starch upon the inclusion of thyme essential oil. The authors attributed this phenomenon to the interactions between the components of the polymeric matrix and the essential oil. In a previous study [1], we explained that the presence of chitosan enhanced the polymer-solvent interactions and decreased the viscosity of the medium as can be seen in Table S2 (Supplementary material).

3.3. Size and morphology of the fibers examined by SEM

The size and morphology of the fibers, which determine the properties of the formulated materials, were analyzed by SEM. The uniformity and fineness of fibers produced during electrospinning of blends of PVA and oil-in-water emulsions were influenced by the viscoelastic behavior of the emulsion and the chain entanglements which is a relevant parameter that also governs the microstructure and morphology of the fibers [44]. By incorporating an appropriate amount of polymer PVA into the continuous phase, the dispersed oil phase droplets were effectively trapped, facilitating the stretching and orientation in both phases.

Table 2
Thermal properties of electrospun PVA-based matrices functionalized with *Mentha piperita* EO obtained by DSC and TGA.

Sample	T_m(°C)	ΔH_{peak1}(J/g)	ΔH_m(J/g)	X_c(%)
PVA	213±1[a]	–	48.2 ± 0.5[b]	29.8 ± 0.3[b]
87.5:12.5	211.9 ± 0.1[a]	3.62 ± 0.07[a]	47.0 ± 1[b]	29.1 ± 0.8[b]
82:18	211.7 ± 0.2[a]	5.48 ± 0.02[b]	41.0±3[a]	26.0 ± 2[a,b]
75:25	213.3 ± 0.1[a]	8.9 ± 0.5[c]	40.0±1[a]	24.6 ± 0.7[a]

[a] Different super index in the same column indicates significant differences among samples ($p < 0.05$).

Fig. 1 shows a more aligned pattern of electrospun nanofibers with increasing amounts of emulsion included in the PVA matrix. A trend of decreasing diameter upon the addition of higher concentrations of emulsion was also observed, with a distribution centered at 300 nm for the 82:18 formulation, showing a nanostructure more homogeneous than other fiber mats. In contrast, the 75:25 sample presented a distribution centered in the range of 300–400 nm, due to the appearance of fused fibers and the formations of ducts, with a lower contribution of the fiber population above 500 nm. These phenomena were probably a consequence of the decrease in viscosity due to the high proportion of emulsion [1].

According to Hadipour-Goudarzi et al. [43], an increase in the viscosity of the fiber-forming solution leads to greater entanglement of polymer chains and higher resistance of the solution to stretching.

3.4. Contact angle

To evaluate the surface hydrophilicity of the samples, the contact angle was analyzed as shown in Fig. 2.

The contact angle of the PVA control had a value characteristic of hydrophilic surfaces. With the addition of the emulsion the mat conserved its hydrophilic feature but with a shift to more hydrophobic character. Specifically, the 75:25 mat showed an increase in the contact angle giving the highest value compared to the PVA control ($p < 0.05$). This phenomenon would indicate the presence of soy lecithin and/or the essential oil on the surface of the fibers. Similar findings were reported by Tang et al. [47], who evaluated the contact angle of a gelatin film loaded with thymol and lecithin, while Hu et al. [48] explained that the increase in the contact angle may be due to a heterogeneous distribution of the hydrophobic compound within a hydrophilic matrix.

Mouro et al. [49] reported that O/W emulsion presented a hydrophilic character due to inherent hydrophilic nature of both PVA and CH. However, the incorporation of the EO became the electrospun fiber mats to a more hydrophobic feature.

3.5. Thermal analysis

Fig. 3 a shows the thermograms with the different thermal events associated performed by DSC.

As can be seen in Fig. 3a, samples functionalized with the active emulsion presented an endothermic event around 150 °C, the ΔH value of which is shown in Table 2. Increasing the emulsion content in the formulation led to an increase in the enthalpy value. This endothermic event could be associated with the loss of essential oil or loss of water bound to chitosan, a component of the emulsion. Finally, the endothermic event at around 211 °C ascribed to the melting of the crystalline phase of PVA was identified [1,50]. In Table 2, the crystallinity degree was calculated from the ΔH melting values by using the equation informed by Kubo et al. [51] and Xing et al. [52]

$$\chi_c = \frac{\Delta H_m}{\Delta H_m^0} \times 100 \quad (2)$$

Where χ_c is the degree of crystallinity, $\Delta H_m$is the melting enthalpy related to the crystalline phase of the polymer sample, and$\Delta H_m^0$is tlhe enthalpy associated with 100 % crystalline PVA, the value of which is 161.6 J/g [52]. As can be seen in Table 2, with the addition of 12.5 % of the emulsion no significant differences were observed in the $\chi_c$values ($p > 0.05$) compared to the control sample PVA indicating that the assembly of active emulsion in this proportion did not produce changes in the crystalline phase of the PVA. On the contrary, greater additions of active emulsions caused a decrease in the melting enthalpy and a consequent a decrease in the crystallinity degree. This fact showed that the greater inclusion of emulsion produced an impediment to the interactions between the PVA chains [51].

The thermal stability of the samples was also examined by TGA analysis. Fig. 3b and c depicts the TGA curves and DTGA profile of the samples, respectively. The TGA of PVA film showed three different weight loss stages; the first weight loss was ascribed to the remotion of water characteristic of the hydrophilicity of the polymers, while the second stage, with a percentage of 80.0 % (Supplementary material Table S3), was assigned to the formation of acetaldehyde and acetic acid due to the deacetylation process [53,54]. The next weight loss event located at 420°-550 °C had a percentage of weight loss of 8.8 %. Two hypotheses could explain the latter stage; the first could be the degradation of a compound of low molecular weight obtained from the scission of the main chain and the other, the degradation of the heavier compounds obtained in the first degradation stage [55].

The addition of the active emulsion produced a significant change in the weight loss profiles. The weight loss in the range of 100°-200 °C (Fig. 3b) and the maximum in DTG curves (Fig. 3c) observed by all samples functionalized with essential oil could be related to the transition observed by DSC. Shetta et al. [56] reported that peppermint essential oil has a weight loss at around 160 °C attributed to the evaporation of volatile compounds of essential oil. It is worth noting that the decomposition of composite matrices began at a higher temperature than those observed for single PVA films, probably due to the improvement in the thermal stability of the PVA:emulsion materials. In detail, the weight of PVA:emulsion was approximately 70 % in a temperature range of 200–420 °C. This effect could be explained by the soy lecithin presence whose carbonyl groups interact with the PVA chains [50]. This same effect was explained by Cristancho et al. [57], who affirmed that the presence of carbonyl generated a reinforcing effect in the PVA matrix owing to an increase in the activation energy. According to Estevez-Areco et al. [58], this result indicates that EO addition delayed the thermal degradation of PVA, suggesting chemical interaction between rosemary components and PVA side chains, supporting the theory that PVA encapsulated and thermally stabilized the EO components. Finally, the inclusion of the emulsion in the nonwoven electrospun matrices caused an increase in the percentage of weight loss, which could be elucidated by the presence of strong interactions between the carbonyl groups of lecithin and the decomposition products obtained at lower temperatures [49].

3.6. Mechanical properties

Fig. 4a and b summarize the mechanical properties (tensile strength and percentage of elongation) of the nanostructured matrices,

As shown in Fig. 4a, the control film demonstrated the highest tensile strength value (10 MPa), and the mat incorporated with the highest amounts of crosslinked emulsion showed the lowest value, which were in general agreement with Li et al. [59]. The assembly of crosslinked emulsion weakened the hydrogen bonding of the PVA, thus disordering the internal network and cohesiveness of the matrix, which resulted in a decrease in stress values, suggesting that the flexibility of these films was much higher than that of the control film (Fig. 4a and b). The lower stress and strain values of the 75:25 formulation could be explained at the microstructure level by the existence of thinner fibers, which correlated with a lower solution viscosity.

The highest strain values were obtained for the 82:18 electrospun matrices with an intermediate content of crosslinked active emulsion, probably due to the combined action of the system components and the contribution of both the essential oil and lecithin to intercalate into the PVA chains. Similar explanations were reported by Li et al. [60]. Consequently, the interactions between the components of the emulsion, essential oil, lecithin, and/or chitosan, facilitated the sliding of the polymeric chains producing an increase in the elongation [50]. In line with these results, Lan et al. [61] observed that high proportions of limonene in electrospun PVA matrices produced an increase in elongation, indicating a plasticizing effect by the active compound.

The profiles depicted in Fig. 4c showed that an increase in emulsion content resulted in a fiber matrix with higher elongation values, up to a

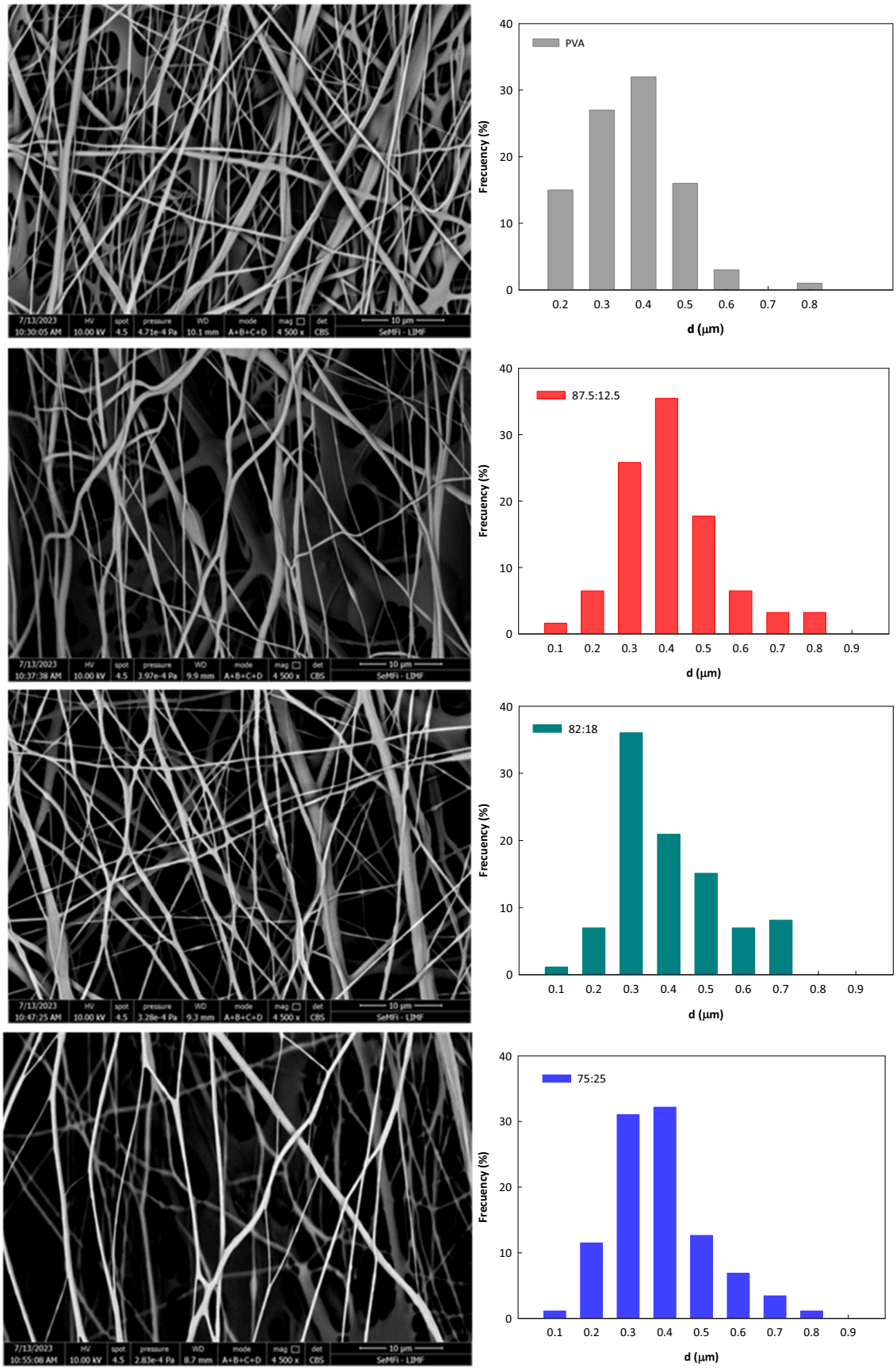

Fig. 1. SEM micrographs of electrospun matrices with different proportions of emulsion: a) PVA, b) 87.5:12.5, c) 82:18, d) 75:25.

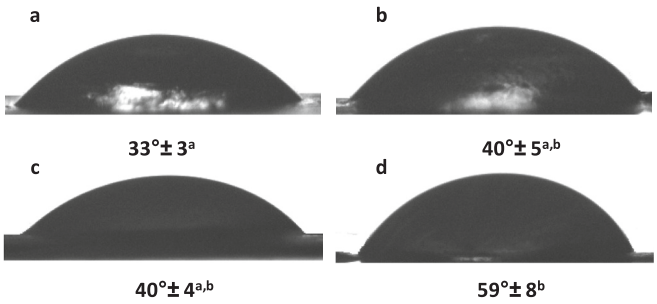

Fig. 2. Contact angle of electrospun matrices based on PVA with different proportions of emulsion (PVA:Em): a) PVA, b) 87.5: 12.5, c) 82:18, d)75:25.

concentration of 25 %. At this concentration, a change in the mechanical behavior was observed, likely due to an excess of emulsion content.

An alternative way to evaluate the mechanical properties of materials was to examine the SEM images of the matrices after they were subjected to mechanical testing (Fig. 5).

SEM images enabled the observation of an orientation pattern of the fibers in the direction of tension [60]. Additionally, the assays caused an increase in fiber fineness. Similar results were reported by Leones et al. [62], who worked with polylactic acid (PLA) matrices obtained by electrospinning.

According to Tarus et al. [63], the mechanical profiles of the functionalized mats, an initial stage of breaking of the adhesion points between the nanofibers upon application of tensile load and a subsequent lid in which the nanofibers slide over each other after all adhesion points have been broken. The authors proposed that the mats composed of thinner non-beaded fibers should have more inter-fiber contact points per unit volume and consequently different mechanical behavior.

The higher adhesion tensile at the inter-nanofiber junctions due to the reduced diameter could explain the increase in the elongation values. In this sense, after the tensile test, it was observed that the fibers of the matrices with a higher proportion of crosslinked emulsion exhibited a marked waviness.

3.7. Dynamic mechanical analysis

Fig. 6 shows the results obtained by DMA analysis, which facilitate the detection of phase transitions and relaxation processes by measuring the solid-state rheological properties of viscoelastic materials as a function of frequency and temperature parameters.

For all formulations tested, the storage modulus values (Fig. 6a) decreased with increasing temperatures. Two characteristic transitions of PVA could be observed: 1) an event located in the range between −4 and 30 °C associated with the β transition, explained by moisture adsorption [64], 2) α relaxation transition identified in the range between 50 and 100 °C ascribed to the glass transition temperature. The increase in the emulsion content generated a decrease in the modulus over the entire temperature range. This fact would be explained by different factors such as modifications in the radius of the fibers which would generate a decrease in the module [64] and/or the disruption of the PVA chain packing structure due to the presence of emulsion [65]. On the other hand, the curves of the tan δ for PVA and 87.5:12.5 samples showed a peak corresponding to Tg located at about 100 °C while for samples with the highest emulsion content, the curves after Tg exhibited a shoulder explained by the presence of a second phase enriched in emulsion components (PVA and chitosan). According to Giannakas et al. [66], this result confirmed the presence of certain immiscibility between the phases without total phase separation among components.

To elucidate the molecular interactions between different compounds of the electrospun matrix, ATR-FTIR spectra were studied.

Different regions of the ATR-FTIR spectrum of PVA are shown in Fig. 7a and b. The absorption maximum centered at 3299 cm^{-1} (Fig. 7a)

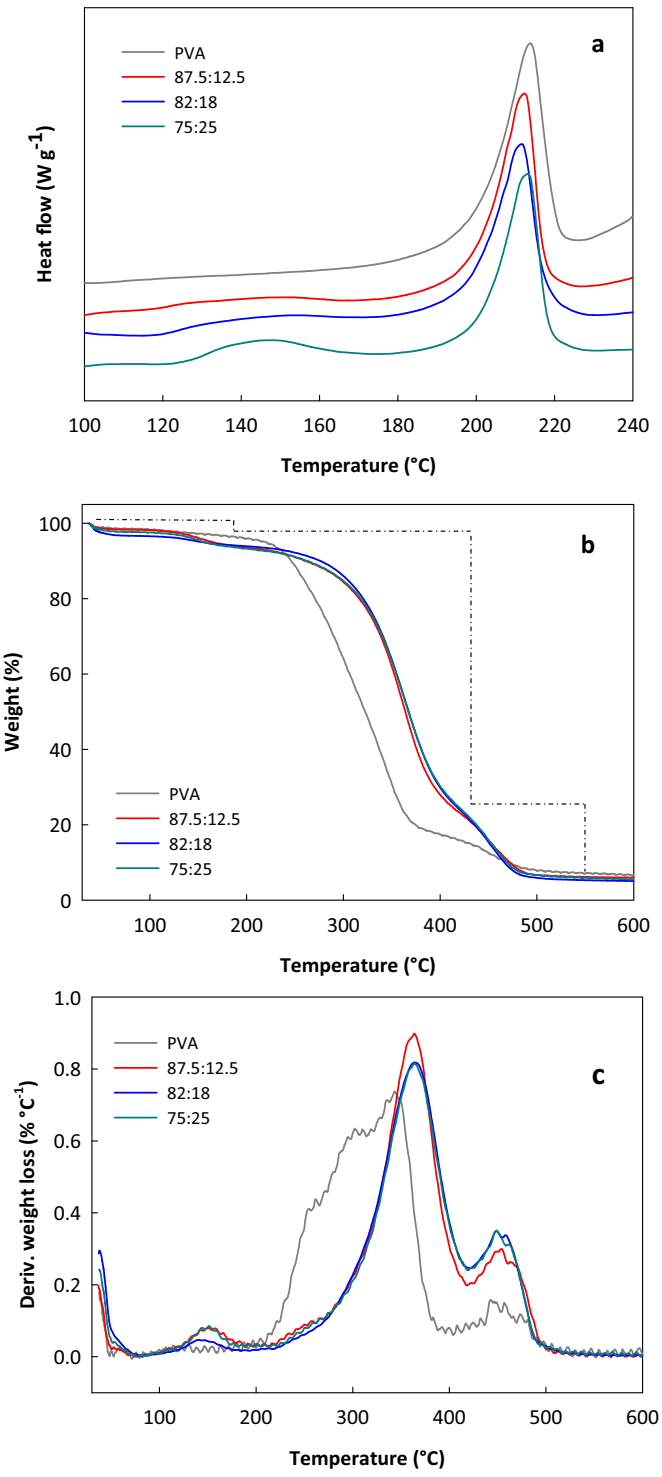

Fig. 3. Thermal analysis of different electrospun matrices functionalized with *Mentha piperita* EO showing: (a) thermograms obtained by DSC, (b) weight loss curves obtained by TGA, and (c) differential weight loss by DTG.

is associated with the stretching of -OH groups characteristics of PVA. Meanwhile, the bands located at 2854 (νAS) and 2920 (νS) cm^{-1} were assigned to symmetric and anti-symmetric CH_2 vibrations of the hydrocarbon chain [67,68]. As can be seen in Fig. 7b, the maximum related to the stretching of carbonyl groups evidenced absorption peaks at 1425 cm^{-1} and the band due to the vibrational deformation of the C—H bond is located at 1322 cm^{-1}, the stretching of the C—O group at 1090 cm^{-1}, and the vibration of the C-O-C ring at 932 cm^{-1} [1,51,69].

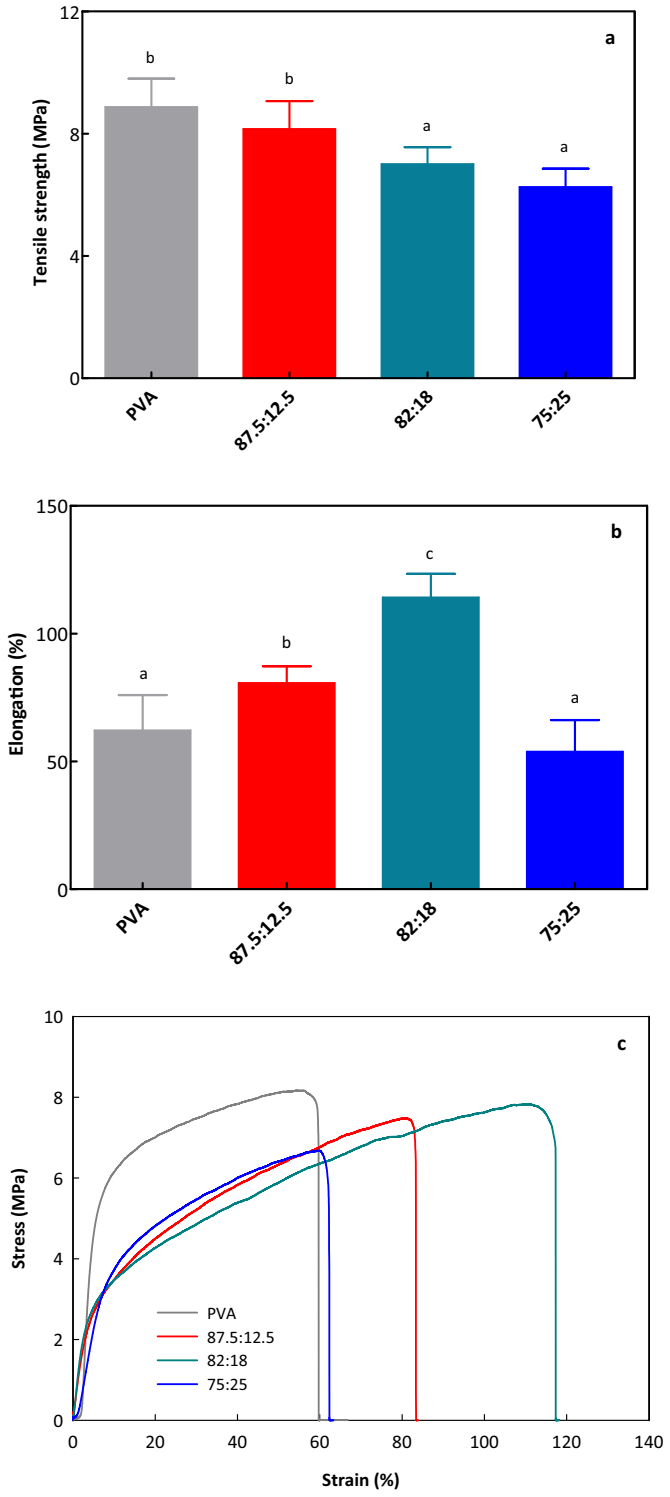

Fig. 4. Mechanical properties of functionalized electrospun matrices based on PVA with different proportions of emulsion (PVA:Em): (a) tensile strength, (b) percentage of elongation. Mechanical profiles of the functionalized electrospun matrices (c).

The addition of the functionalized emulsions with *Mentha piperita* EO produced modifications of vibrational bands, specifically a shift of the peak associated with the stretching of -OH to a higher wavelength indicating the increase in hydrogen bridge-type interactions [70] (Fig. 7a). On the other hand, the changes in the 3000–2800 cm^{-1} region were evident. These modifications could be attributed to the presence of lecithin on the surface of the fibers. Also, the appearance of a new peak located at 2856 cm^{-1}, intensified with the increase of the proportion of the emulsion, was consistent with the absorption peak of the soy lecithin. This finding would indicate its presence on the surface of nanofibers in concordance with contact angle results. Fig. 7 shows that the increase in the emulsion content correlated with the increase in the intensity of the absorption band at 1742 cm^{-1} ascribed to C═O stretching vibration of carbonyl groups of phosphatidylcholine, and 1234 cm^{-1} (P═O stretching vibration) linked to the presence of lecithin on the surface [50]. After the formation of the composite emulsion, the peak at 1234 cm^{-1} (P═O) was shifted to 1248 cm^{-1}. This phenomenon could be due to the interactions between the chitosan and the P═O bond of phospholipids during the formation of complexes [71]. All results would indicate that the essential oil was completely encapsulated.

Spectral window 12009–00 cm^{-1} associated with the fingerprint of the polymer did not undergo modifications with the addition of the EO.

Emulsions were prepared using chitosan, PVA (polyvinyl alcohol), and lecithin functionalized with peppermint essential oil. The emulsions were crosslinked with sodium citrate. The optimization process considered the zeta potential and size of the nanoparticles. The best results were obtained for Em_{10}, which was prepared using 10 % (w/w) soy lecithin.

The concentration of lecithin capable of emulsifying peppermint essential oil was selected to obtain cross-linked emulsions with sodium citrate. The influence of the cross-linked emulsion ratio on the rheological properties, thermal behavior, mechanical properties, and fiber morphology was comprehensively analyzed in detail. In this sense, precise control of the emulsion properties is required to achieve the desired result of the nanofibers for wound dressing application.

In summary, the selected emulsion (Em_{10}) was mixed with 16 % PVA in different proportions to produce fiber-forming suspensions (Supplementary material, Fig. S2). The ratios used were 87.5:12.5, 82:18, and 75:25. The fiber-forming suspensions were processed by electrospinning using a rotating drum which allowed the production of aligned fibers (Supplementary material, Fig. S2).

The polymer concentration and the incorporation of oil-in-water emulsions were adjusted to obtain fibers with customized diameters and with different degrees of adhesion and interconnection between nanofibers, which had an impact on mechanical behavior.

As is well known, PVA is an environmentally friendly material with good rheological and mechanical properties capable of forming mats by electrospinning.

Different properties of the electrospun matrices were evaluated to select the best mat for topical applications. The interactions between the components were evinced using ATR-FTIR (attenuated total reflectance Fourier transform infrared spectroscopy) observing the appearance of peaks and shifts as a result of the assembly of cross-linked emulsions.

The close interactions established would be confirmed through thermal analysis where the appearance of a single Tg indicated compatibility since the appearance of separate phases could not be observed for 87.5:12.5 sample while for samples with the highest emulsion content, the curves underwent a splitting due to the appearance of two phase, one rich in the emulsion and the other in PVA. A broadening of the alpha relaxation as well as a shift of the beta towards lower temperatures were also observed. TGA analysis unveiled the thermal protection and stabilization of the PVA in the emulsion functionalized with peppermint EO.

The composite matrices retained their hydrophilic character, which is desirable for topical application as dressings, but with a slight increase in hydrophobicity due to the presence of the lecithin and the essential oil as was observed by contact angle.

Mechanical tests were conducted to evaluate the properties of the electrospun matrices. Despite the inclusion of emulsions, the PVA maintained or improved its elasticity due to the influence of fiber orientation.

Based on the evaluation of the results, the 82:18 ratio of PVA to Em_{10}

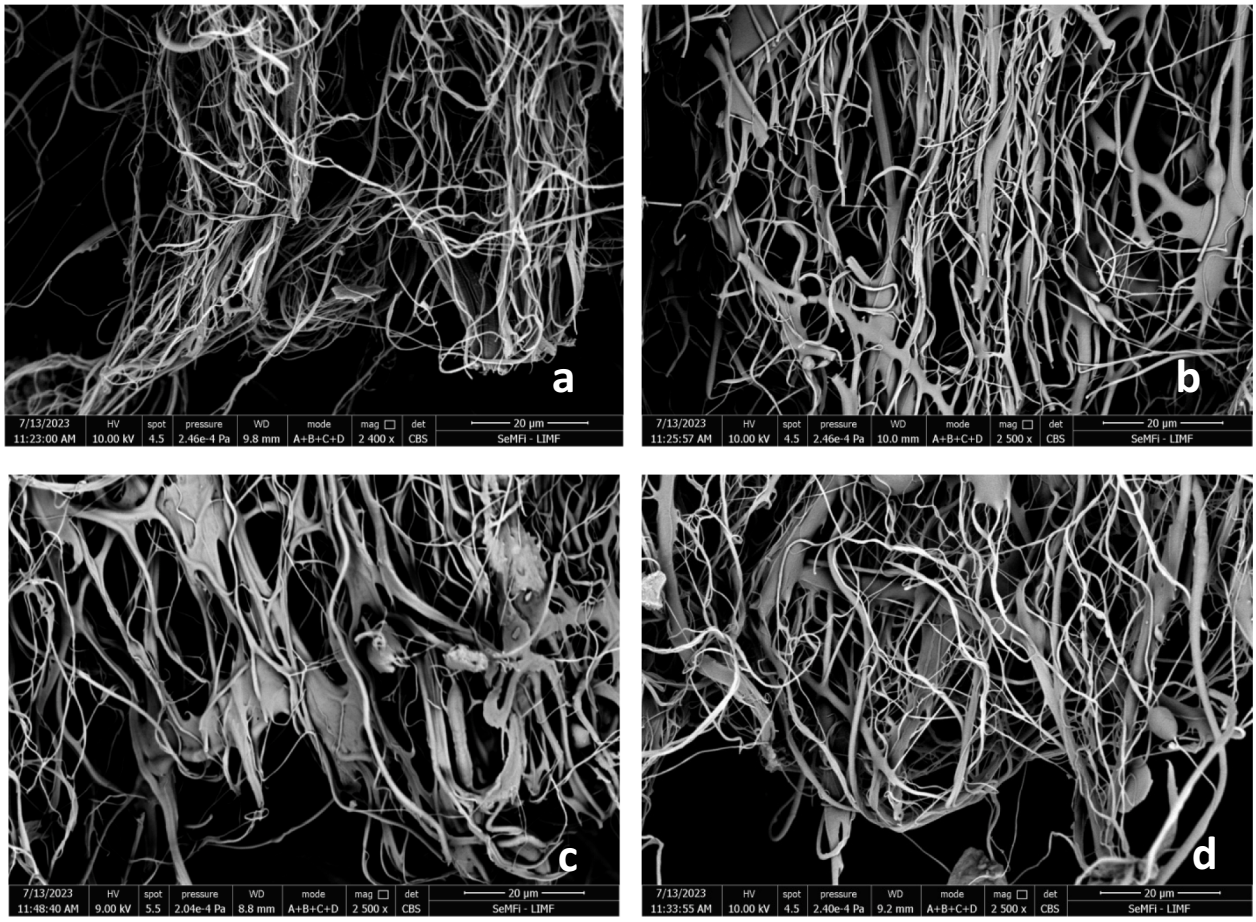

Fig. 5. SEM micrographs of the matrices functionalized with *Mentha piperita* EO submitted to tension tests: a) PVA, b) 87.5: 12.5, c) 82:18, and d) 75:25.

was selected for its high EO content. This formulation was deemed suitable for subsequent skin release studies.

3.8. Diffusion of peppermint EO by CLSM and ATR-FTIR

To conduct the experiments of diffusion, porcine skin explants were put in close contact with 82:18 samples for 1 and 7 h. Then, based on the intrinsic fluorescence of the peppermint EO, its diffusion in the porcine explant was monitored by using CSLM at 275 nm, generating a maximum emission near 341 nm. To analyze the penetration of essential oil through the skin, histological slices were examined. Fig. 8a shows the image of the control skin without any contact with the EO, revealing no fluorescence signal. Therefore, the ear porcine skin showed no interference in the signal. The histological section of the sample after 1 h of contact (Fig. 8b) put in evidence the location of the essential oil mainly on the surface of the *stratum corneum* (SC).

On the other hand, after 7 h of contact with the matrix containing the EO, the distribution of the drug throughout the viable epidermis was observed (Fig. 8c).

These results were supported by 3D images obtained by optical sectioning (Supplementary material, Fig. S3a and b), showing the distribution of the essential oil distribution across the different layers of the skin. These results agreed with previous studies reported by Lamarra et al. [38]. The authors observed that the penetration of cabreuva essential oil increased over time, indicating the penetration ability of this essential oil which could be related to the chemical structure of trans-nerolidol, the main compound of cabreuva essential oil.

After contact with the skin specimen for 7 h, functionalized electrospun retained its ability to release the EO. Menthol, the major constituent of peppermint, permeates the epidermis which would improve the accessibility of other drugs [72]. According to Kamatou et al. [73], limonene and menthol are effective transdermal penetration enhancers. These compounds enhance the percutaneous absorption by reversibly perturbing the permeability barrier of the SC. Fox et al. [74] suggested disruption of the hydrogen bonding network at the ceramid heads as a likely mechanism for enhancing the permeation of the drug through the skin.

Three mechanisms would explain the enhancement in drug permeation through the skin. These include the increase in drug diffusivity in the SC, disruption of the ordered lipid structure of the SC, and the increase in the electrical conductivity of tissues [73].

Studies conducted showed that menthol prompts the disruption of SC lipid assembly comparable to that caused by heat, demonstrating that it can act as a fluidizer [75].

In addition, phospholipids have structural and chemical properties that can also alter lipid packing in the SC and can therefore be used in skin permeability applications. Phospholipids can easily intercalate into packed lipids or promote hydrogen bonding with polar head groups acting as fluidizers with minimal adverse effects on skin structure [75].

Fig. 8d and e summarizes the ATR-FTIR spectra of the control skin explants (without treatment) along with the skin sample measured after 1 h of impregnation with the EO or the emulsion and after 1 and 7 h of close contact with electrospun mats, respectively.

Fig. 8d shows the spectral region between 3000 and 2800 cm^{-1}, where the peaks at 2850 cm^{-1} and 2920 cm^{-1} were attributed to the presence of long alkyl chains that are components of cholesterol, ceramides, and fatty acids, which are the main components of the stratum corneum [21]. The addition of essential oil produced a shift in the peak associated with the symmetric stretch from 2850 cm^{-1} to 2870 cm^{-1}, while the maximum associated with the antisymmetric stretching

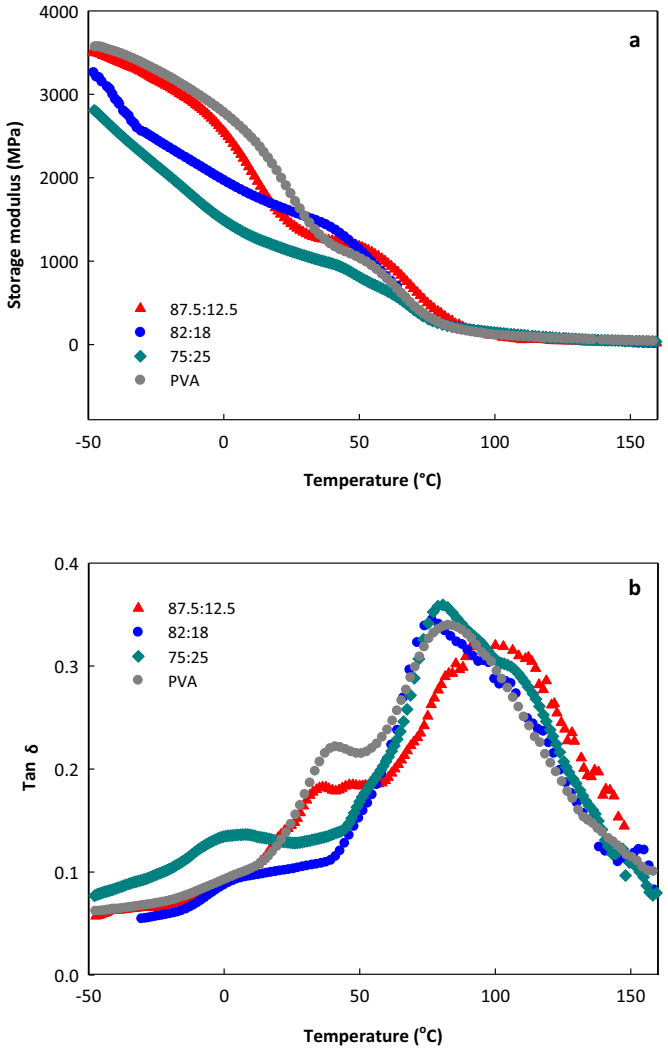

Fig. 6. Dynamic mechanical spectra of electrospun matrices functionalized with *Mentha piperita* essential oil stabilized in a chitosan-based emulsion: a) storage modulus and b) tan delta.

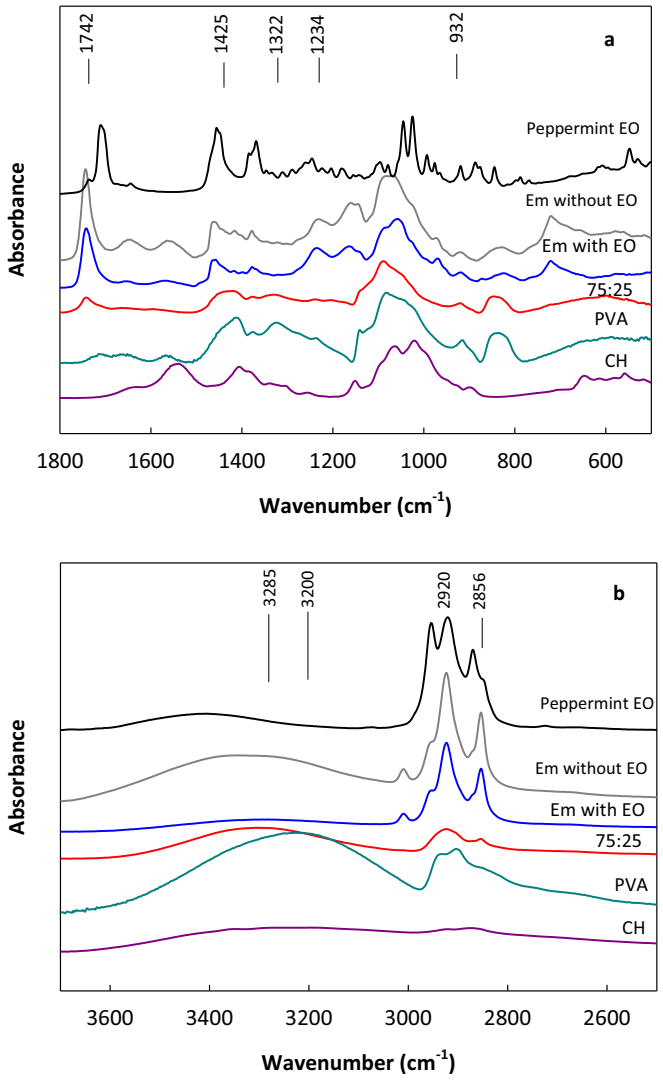

Fig. 7. ATR-FTIR spectra of electrospun matrices functionalized with *Mentha piperita* essential oil showing different regions: a) 1800 - 500 cm^{-1} and b) 3500 - 2500 cm^{-1}.

also showed a shift towards higher wavenumbers.

This shift was associated with an increase in the disorder of the lipophilic chains present in the SC [21,76], indicating an enhancement in the fluidity of the lipid membranes. According to Ma et al. [68], the red shift in these vibrations indicates a conformational change from gauche to trans, while Boncheva et al. [77] reported that this change corresponds to the structural modification of the string arrangement from an orthorhombic or hexagonal to a liquid crystal-like phase. A change in wavenumber was also observed for samples in contact with the emulsion, but to a lesser extent than for samples in direct contact with the EO. On the other hand, a localized peak at 3000 cm^{-1} was visualized, attributed to the presence of lecithin.

Fig. 8e compares the untreated control explant and the skin samples after 1 and 7 h of close contact with the functionalized 82:18 electrospun mat. The sample in close contact with the electrospun matrix for 1 h did not show any significant differences concerning the control, while after 7 h, an attenuation of the signals with a widening of the peaks was observed. According to the explanations provided by several authors, this behavior could be explained by the extraction of lipids from the SC [76,78]. On the other hand, the broadening of the peaks gave signals of structural disorganization of the lipophilic chains [79].

4. Conclusions

The electrospinning technique was adequate to obtain a nonwoven PVA-based matrix capable of including an emulsion composed of chitosan and peppermint essential oil (*Mentha piperita*) as an active agent, establishing interactions between the components as supported by ATR-FTIR technique. The electrospinning instrument coupled to a rotary drum collector allowed the fabrication of aligned nanofibers. Although the incorporation of the functionalized emulsion, the mechanical properties and the structural integrity were preserved in relation to the single PVA matrix.

The diffusion of the active agent from the 82:18 electrospun matrices to porcine skin explants was detected by confocal microscopy taking advantage of the fluorescence of the *Mentha piperita*. The EO caused a structural disorganization of the lipophilic chains of the stratum corneum as supported by ATR-FTIR. Specifically, the presence of menthol prompted a disorder of SC lipid assembly demonstrating that it can act as a fluidizer.

Tailored electrospun matrices would have potential applications as devices for topical or transdermal treatments due to their vehiculization role that allows the diffusion of peppermint essential oil as a skin penetration enhancer.

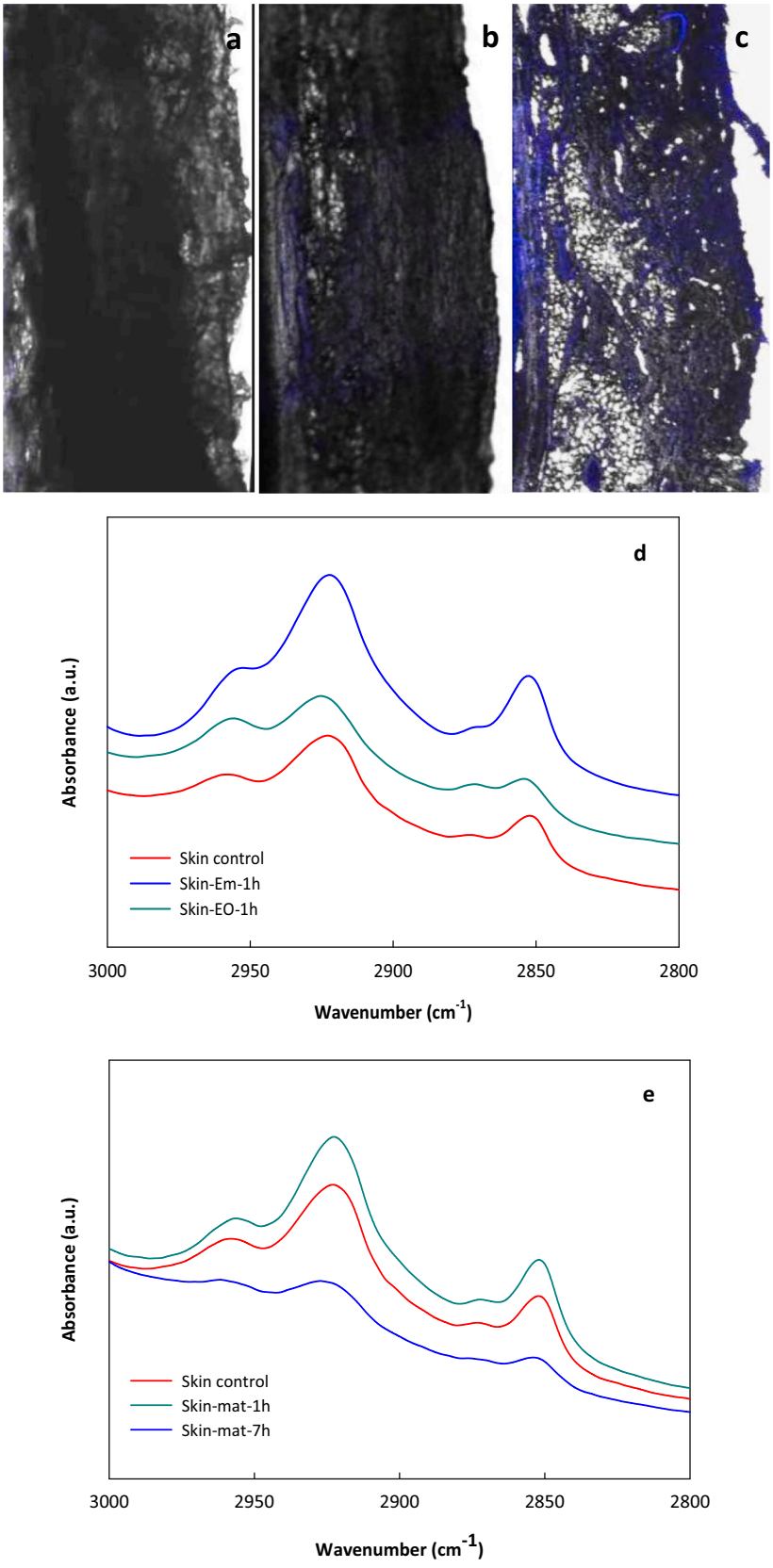

Fig. 8. Histological sections of ear porcine skin of a control explant (a), and explants after being in contact with 82:18 electrospun matrices functionalized with *Mentha piperita* for 1 h (b) and 7 h (c). ATR-FTIR spectra of ear porcine skin explants after 1 h of impregnation with: (d) the active emulsion and *Mentha piperita* essential oil and (e) after 1 and 7 h of close contact with 82:18 electrospun mats. Spectral range: 3000–2800 cm^{-1}.

CRediT authorship contribution statement

J.L.: Methodology, investigation, writing-review. S.R.: Writing-original draft, formal analysis, writing-review & editing. A.P.: Writing-original draft, formal analysis, writing-review & editing, funding acquisition. D.L.: Writing-original draft, writing-review & editing, funding acquisition. All authors have approved the final version of the manuscript.

Declaration of competing interest

The authors declare that they have no known competing financial interests or personal relationships that could have appeared to influence the work reported in this paper.

Data availability

Data will be made available on request.

Acknowledgments

This work was supported by the Argentinean Agency for the Scientific and Technological Promotion (ANPCyT) (Projects PICT 2019-02008 and PICT 2019-03380). Project PID2021-123753NB-C31 funded by MCIN/AEI/10.13039/501100011033 and, by "ERDF A way of making Europe", by the "European Union".

Appendix A. Supplementary data

Supplementary data to this article can be found online at https://doi.org/10.1016/j.ijbiomac.2023.125980.

References

[1] J. Lamarra, M.N. Calienni, S. Rivero, A. Pinotti, Electrospun nanofibers of poly (vinyl alcohol) and chitosan-based emulsions functionalized with cabreuva essential oil, Int. J. Biol. Macromol. 160 (2020) 307–318, https://doi.org/10.1016/j.ijbiomac.2020.05.096.
[2] E. Mele, Electrospinning of essential oils, Polymers (Basel) 12 (4) (2020) 908, https://doi.org/10.3390/polym12040908.
[3] M. Ghasemi, M.A. Miri, M.A. Najafi, M. Tavakoli, T. Hadadi, Encapsulation of Cumin essential oil in zein electrospun fibers: characterization and antibacterial effect, J. Food Meas. Charact. 16 (2) (2022) 1613–1624, https://doi.org/10.1007/s11694-021-01268-z.
[4] M. Gagaoua, V.Z. Pinto, G. Göksen, L. Alessandroni, M. Lamri, A.L. Dib, F. Boukid, Electrospinning as a promising process to preserve the quality and safety of meat and meat products, Coatings 12 (5) (2022) 644, https://doi.org/10.3390/coatings12050644.
[5] G. Maleki, E.J. Woltering, M.R. Mozafari, Applications of chitosan-based carrier as an encapsulating agent in food industry, Trends Food Sci. Technol. 120 (2022) 88–99, https://doi.org/10.1016/j.tifs.2022.01.001.
[6] S. Anjum, F. Rahman, P. Pandey, D.K. Arya, M. Alam, P.S. Rajinikanth, Q. Ao, Electrospun biomimetic nanofibrous scaffolds: a promising prospect for bone tissue engineering and regenerative medicine, Int. J. Mol. Sci. 23 (16) (2022) 9206, https://doi.org/10.3390/ijms23169206.
[7] A. Haider, S. Haider, I.K. Kang, A comprehensive review summarizing the effect of electrospinning parameters and potential applications of nanofibers in biomedical and biotechnology, Arab. J. Chem. 11 (8) (2018) 1165–1188.
[8] B. Zaarour, L. Zhu, X. Jin, A review on the secondary surface morphology of electrospun nanofibers: formation mechanisms, characterizations, and applications, Chem. Select. 5 (4) (2020) 1335–1348, https://doi.org/10.1002/slct.201903981.
[9] W.E. Teo, S. Ramakrishna, A review on electrospinning design and nanofibre assemblies, Nanotech. 17 (14) (2006) R89. opscience.iop.org. https://doi.org/10.1088/0957-4484/17/14/R01/meta.
[10] S. Thenmozhi, N. Dharmaraj, K. Kadirvelu, H.Y. Kim, Electrospun nanofibers: new generation materials for advanced applications, Mater. Sci. Eng. B 217 (2017) 36–48, https://doi.org/10.1016/j.mseb.2017.01.001.
[11] C.Y. Xu, R. Inai, M. Kotaki, S. Ramakrishna, Aligned biodegradable nanofibrous structure: a potential scaffold for blood vessel engineering, Biomater. 25 (5) (2004) 877–886, https://doi.org/10.1016/S0142-9612(03)00593-3.
[12] P. Nitti, N. Gallo, L. Natta, F. Scalera, B. Palazzo, A. Sannino, F. Gervaso, Influence of nanofiber orientation on morphological and mechanical properties of electrospun chitosan mats, J. Health. Eng. 2018 (2018), https://doi.org/10.1155/2018/3651480.
[13] M. Eslamian, M. Khorrami, N. Yi, S. Majd, M.R. Abidian, Electrospinning of highly aligned fibers for drug delivery applications, J. Mater. Chem. B 7 (2019) 224–232, https://doi.org/10.1039/C8TB01258J.
[14] A.J. Robinson, A. Pérez-Nava, S.C. Ali, J.B. González-Campos, J.L. Holloway, E. M. Cosgriff-Hernandez, Comparative analysis of fiber alignment methods in electrospinning, Matter. 4 (3) (2021) 821–844, https://doi.org/10.1016/j.matt.2020.12.022.
[15] M.A.A. Shahid, M.N. Ali, S. Uddin, S.M. Miah, M. Islam, M.S.I. Jamal Mohebbullah, Antibacterial wound dressing electrospun nanofibrous material from polyvinyl alcohol, honey and Curcumin longa extract, J. Ind. Text. 51 (3) (2020) 455–469, https://doi.org/10.1177/1528083720904379.
[16] J. Jalvandi, M. White, Y. Gao, Y.B. Truong, R. Padhye, I.L. Kyratzis, Polyvinyl alcohol composite nanofibres containing conjugated levofloxacin-chitosan for controlled drug release, Mater. Sci. Eng. C (2017) 73440–73446, https://doi.org/10.1016/j.msec.2016.12.112.
[17] T. Tadros, Viscoelastic properties of sterically stabilised emulsions and their stability, Adv. Colloid Interf. Sci. 222 (2015) 692–708, https://doi.org/10.1016/j.cis.2015.03.001.
[18] M.S. Morais, D.P. Bonfim, M.L. Aguiar, W.P. Oliveira, Electrospun poly (vinyl alcohol) nanofibrous mat loaded with green propolis extract, chitosan and nystatin as an innovative wound dressing material, J. Pharm. Innov. (2022) 1–15, https://doi.org/10.1007/s12247-022-09681-7.
[19] D. Coelho, B. Veleirinho, L. Mazzarino, T. Alberti, E. Buzanello, R.E. Oliveira, R. A. Yunes, M. Moraes, M. Steindel, M. Maraschin, Polyvinyl alcohol-based electrospun matrix as a delivery system for nanoemulsion containing chalcone against Leishmania (Leishmania) amazonensis, Colloids Surf. B 198 (2021), 111390, https://doi.org/10.1016/j.colsurfb.2020.111390.
[20] W. Zhang, H. Jiang, J.W. Rhim, J. Cao, W. Jiang, Effective strategies of sustained release and retention enhancement of essential oils in active food packaging films/coatings, Food Chem. (2022) 367130671, https://doi.org/10.1016/j.foodchem.2021.130671.
[21] A. Nowak, W. Duchnik, E. Makuch, L. Kucharski, P. Ossowicz-Rupniewska, K. Cybulska, T. Sulikowski, M. Moritz, A. Klimowicz, *Epilobium angustifolium* L. essential oil—biological activity and enhancement of the skin penetration of drugs—in vitro study, Molecules 26 (23) (2021) 7188, https://doi.org/10.3390/molecules26237188.
[22] O. Taylan, N. Cebi, O. Sagdic, Rapid screening of Mentha spicata essential oil and L-menthol in Mentha piperita essential oil by ATR-FTIR spectroscopy coupled with multivariate analyses, Foods 10 (2) (2021) 202, https://doi.org/10.3390/foods10020202.
[23] I. Liakos, L. Rizzello, H. Hajiali, V. Brunetti, R. Carzino, P.P. Pompa, A. Athanassiou, E. Mele, Fibrous wound dressings encapsulating essential oils as natural antimicrobial agents, J. Mater. Chem. B 3 (2015) 1583–1589, https://doi.org/10.1039/C4TB01974A.
[24] J.F. Mendes, L.B. Norcino, T.Q. Corrêa, T.V. Barbosa, R.T. Paschoalin, L.H. C. Mattoso, Obtaining poly (lactic acid) nanofibers encapsulated with peppermint essential oil as potential packaging via solution-blow-spinning, Int. J. Biol. Macromol. 230 (2023), 123424, https://doi.org/10.1016/j.ijbiomac.2023.123424.
[25] S. García-Salinas, M. Evangelopoulos, E. Gámez-Herrera, M. Arruebo, S. Irusta, F. Taraballi, G. Mendoza, E. Tasciotti, Electrospun anti-inflammatory patch loaded with essential oils for wound healing, Int. J. Pharm. 577 (2020), 119067, https://doi.org/10.1016/j.ijpharm.2020.119067.
[26] N.T. Ardekani, M. Khorram, K. Zomorodian, S. Yazdanpanah, H. Veisi, H. Veisi, Evaluation of electrospun poly (vinyl alcohol)-based nanofiber mats incorporated with Zataria multiflora essential oil as potential wound dressing, Int. J. Biol. Macromol. 125 (2019) 743–750, https://doi.org/10.1016/j.ijbiomac.2018.12.085.
[27] D. Wang, Z. Sun, J. Sun, F. Liu, L. Du, D. Wang, Preparation and characterization of polylactic acid nanofiber films loading Perilla essential oil for antibacterial packaging of chilled chicken, Int. J. Biol. Macromol. 192 (2021) 379–388, https://doi.org/10.1016/j.ijbiomac.2021.09.190.
[28] M.P. Mani, A.A.M. Faudzi, S. Ramakrishna, A.F. Ismail, S.K. Jaganathan, N. Tucker, R. Rathanasamy, Sustainable electrospun materials with enhanced blood compatibility for wound healing applications–a mini review, Curr. Opin. Biomed. Eng. (2023), 100457, https://doi.org/10.1016/j.cobme.2023.100457.
[29] F. Kayaci, T. Uyar, Encapsulation of vanillin/cyclodextrin inclusion complex in electrospun polyvinyl alcohol (PVA) nanowebs: prolonged shelf-life and high temperature stability of vanillin, Food Chem. 133 (3) (2012) 641–649, https://doi.org/10.1016/j.foodchem.2012.01.040.
[30] E. Hebishy, L. Collette, P. Iheozor-Ejiofor, B.A. Onarinde, Stability and antimicrobial activity of lemongrass essential oil in nanoemulsions produced by high-intensity ultrasounds and stabilized by soy lecithin, hydrolyzed whey proteins, gum Arabic, or their ternary admixture, J. Food Process. Preserv. 46 (10) (2022), e16840, https://doi.org/10.1111/jfpp.16840.
[31] N.S. Yussof, T.C. Ping, T.T. Boon, U. Utra, M.E. Ramli, Influence of soy lecithin and sodium caseinate on the stability and in vitro bioaccessibility of lycopene nanodispersion, Food Technol. Biotechnol. 61 (1) (2023) 39–50.
[32] S. Mun, E. Decker, D. McClements, Influence of droplet characteristics on the formation of oil-in-water emulsions stabilized by surfactant– chitosan layers, Langmuir 21 (14) (2005) 6228–6234, https://doi.org/10.1021/la050502w.
[33] G.A. Martău, M. Mihai, D.C. Vodnar, The use of chitosan, alginate, and pectin in the biomedical and food sector—biocompatibility, bioadhesiveness, and biodegradability, Polymers 11 (11) (2019) 1837, https://doi.org/10.3390/polym11111837.
[34] L. Meyer-Déru, G. David, R. Auvergne, Chitosan chemistry review for living organisms encapsulation, Carbohyd, Polym. (2022), 119877, https://doi.org/10.1016/j.carbpol.2022.119877.

[35] S. Das, A.K. Chaudhari, V.K. Singh, A.K.A.K. Dwivedy, N.K. Dubey, Chitosan based encapsulation of Valeriana officinalis essential oil as edible coating for inhibition of fungi and aflatoxin B1 contamination, nutritional quality improvement, and shelf life extension of Citrus sinensis fruits, Int. J. Biol. Macromol. 233 (2023), 123565, https://doi.org/10.1016/j.ijbiomac.2023.123565.
[36] P. Gupta, S. Preet, N. Singh, Preparation of Thymus vulgaris (L.) essential oil nanoemulsion and its chitosan encapsulation for controlling mosquito vectors, Sci. Rep. 12 (1) (2022) 1–14.
[37] M.C. Izquierdo, C.R. Lillo, P. Bucci, G.E. Gomez, L.S.D.V. Martínez, M. Alonso, N. Calienni, J. Montanari, Comparative skin penetration profiles of formulations including ultradeformable liposomes as potential nanocosmeceutical carriers, J. Cosmet. Derm. 19 (11) (2020) 3127–3137, https://doi.org/10.1111/jocd.13410.
[38] J. Lamarra, P. Bucci, L. Giannuzzi, J. Montanari, S. Rivero, A. Pinotti, Biomaterial-based dressings as vehicle for chitosan-encapsulated cabreuva essential oil: cytotoxicity and regenerative activity, React. Funct. Polym. 156 (2020), 104728, https://doi.org/10.1016/j.reactfunctpolym.2020.104728.
[39] P. Bucci, M.J. Prieto, L. Milla, M.N. Calinni, L. Martinez, V. Rivarola, S. Alonso, J. Montanari, Skin penetration and UV-damage prevention by nanoberries, J. Cosmet. Derm. (2017) 1–11, https://doi.org/10.1111/jocd.12436.
[40] J. Lamarra, S. Rivero, A. Pinotti, Design of chitosan-based nanoparticles functionalized with gallic acid, Mater. Sci. Eng. C 67 (2016) 717–726, https://doi.org/10.1016/j.msec.2016.05.072.
[41] M. Al-Remawi, A. Elsayed, I. Maghrabi, M. Hamaidi, N. Jaber, Chitosan/lecithin liposomal nanovesicles as an oral insulin delivery system, Pharm. Dev. Technol. 22 (3) (2017) 390–398, https://doi.org/10.1080/10837450.2016.1213745.
[42] J. Andrade, C. González-Martínez, A. Chiralt, Liposomal encapsulation of carvacrol to obtain active poly (vinyl alcohol) films, Molecules 26 (6) (2021) 1589, https://doi.org/10.3390/molecules26061589.
[43] E. Hadipour-Goudarzi, M. Montazer, M. Latifi, A.A. Aghaji, Electrospinning of chitosan/sericin/PVA nanofibers incorporated with in situ synthesis of nano silver, Carbohydr. Polym. 113 (2014) 231–239, https://doi.org/10.1016/j.carbpol.2014.06.082.
[44] J. Pal, D. Wu, M. Hakkarainen, R.K. Srivastava, The viscoelastic interaction between dispersed and continuous phase of PCL/HA-PVA oil-in-water emulsion uncovers the theoretical and experimental basis for fiber formation during emulsion electrospinning, Eur.Polym.J. 96 (2017) 44–54, https://doi.org/10.1016/j.eurpolymj.2017.09.004.
[45] S. Higashi, T. Hirai, M. Matsubara, H. Yoshida, A. Beniya, Dynamic viscosity recovery of electrospinning solution for stabilizing elongated ultrafine polymer nanofiber by TEMPO-CNF, Sci. Rep. 10 (1) (2020) 13427, https://doi.org/10.1038/s41598-020-69136-2.
[46] L.M. Fonseca, M. Radünz, H.C. dos Santos Hackbart, F.T. da Silva, T.M. Camargo, G.P. Bruni, J.L.F. Monks, E. da Rosa Zavareze, A.R. Dias, Electrospun potato starch nanofibers for thyme essential oil encapsulation: antioxidant activity and thermal resistance, J. Sci. Food Agric. 100 (11) (2020) 4263–4271, https://doi.org/10.1002/jsfa.10468.
[47] Y. Tang, Y. Zhou, X. Lan, D. Huang, T. Luo, J. Ji, Z. Manfang, X. Miao, H. Wang, W. Wang, Electrospun gelatin nanofibers encapsulated with peppermint and chamomile essential oils as potential edible packaging, J. Agric. Food Chem. 67 (8) (2019) 2227–2234, https://doi.org/10.1021/acs.jafc.8b06226.
[48] X. Hu, X. Wang, S. Li, W. Zhou, W. Song, Antibacterialelectrospunpolyvinylalcohol nanofibers encapsulating Berberine-Hydroxypropyl-β-Cyclodextrin inclusion complex, J. Drug Deliv. Sci. Technol. 64 (2021), 102649, https://doi.org/10.1016/j.jddst.2021.102649.
[49] C. Mouro, M. Simões, I.C. Gouveia, Emulsion electrospun fiber mats of PCL/PVA/chitosan and eugenol for wound dressing applications, Adv. Polym. Technol. (2019) 1–11, https://doi.org/10.1155/2019/9859506.
[50] J. Andrade, C. González-Martínez, A. Chiralt, The incorporation of carvacrol into poly (vinyl alcohol) films encapsulated in lecithin liposomes, Polymers 12 (2) (2020) 497, https://doi.org/10.3390/polym12020497.
[51] S. Kubo, J.F. Kadla, The formation of strong intermolecular interactions in immiscible blends of poly (vinyl alcohol) (PVA) and lignin, Biomacromol. 4 (3) (2003) 561–567, https://doi.org/10.1021/bm025727p.
[52] C. Xing, X. Xu, L. Song, X. Wang, B. Li, K. Guo, β-Cyclodextrin-based poly (vinyl alcohol) bibers for sustained release of fragrances, Polymers 14 (2022) 2002, https://doi.org/10.3390/polym14102002.
[53] Z. Peng, L.X. Kong, A thermal degradation mechanism of polyvinyl alcohol/silica nanocomposites, Polym. Degrad. Stab. 92 (6) (2007) 1061–1071, https://doi.org/10.1016/j.polymdegradstab. 2007.02.012.
[54] J. Lamarra, S. Rivero, A. Pinotti, Functionalyzed biomaterials based on poly (vinyl alcohol) and chitosan as a vehicle for controlled release of cabreuva essential oil, Polym. Eng. Sci. (2022), https://doi.org/10.1002/pen.26062 (621-16).
[55] J. Andrade, C. González-Martínez, A. Chiralt, Effect of carvacrol in the properties of films based on poly (vinyl alcohol) with different molecular characteristics, Polym. Degrad. Stab. 179 (2020), 109282, https://doi.org/10.1016/j.polymdegradstab.2020.109282.
[56] A. Shetta, J. Kegere, W. Mamdouh, Comparative study of encapsulated peppermint and green tea essential oils in chitosan nanoparticles: encapsulation, thermal stability, in-vitro release, antioxidant and antibacterial activities, Int. J. Biol. Macromol. 126 (2019) 731–742, https://doi.org/10.1016/j.ijbiomac.2018.12.161.
[57] D. Cristancho, Y. Zhou, R. Cooper, D. Huitink, F. Aksoy, Z. Liu, H. Liang, J. M. Seminario, Degradation of polyvinyl alcohol under mechanothermal stretching, J. Mol. Model. 19 (8) (2013) 3245–3253, https://doi.org/10.1007/s00894-013-1828-6.
[58] S. Estevez-Areco, L. Guz, R. Candal, S. Goyanes, Release kinetics of rosemary (Rosmarinus officinalis) polyphenols from polyvinyl alcohol (PVA) electrospun nanofibers in several food stimulants, Food Packag. Shelf Life 18 (2018) 42–50, https://doi.org/10.1016/j.fpsl.2018.08.006.
[59] C. Li, X. Luo, L. Li, Y. Cai, X. Kang, P. Li, Carboxymethyl chitosan-based electrospun nanofibers with high citral-loading for potential anti-infection wound dressings, Int. J. Biol. Macromol. 209 (2022) 344–355.
[60] X. Li, X. Yang, H. Deng, Y. Guo, J. Xue, Gelatin films incorporated with thymol nanoemulsions: physical properties and antimicrobial activities, Int. J. Biol. Macromol. 150 (2020) 161–168, https://doi.org/10.1016/j.ijbiomac.2020.02.066.
[61] W. Lan, X. Liang, W. Lan, S. Ahmed, Y. Liu, W. Qin, Electrospun polyvinyl alcohol/d-limonene fibers prepared by ultrasonic processing for antibacterial active packaging material, Molecules 24 (4) (2019) 767, https://doi.org/10.3390/molecules24040767.
[62] A. Leones, A. Sonseca, D. López, S. Fiori, L. Peponi, Shape memory effect on electrospun PLA-based fibers tailoring their thermal response, Eur. Polym. J. 117 (2019) 217–226, https://doi.org/10.1016/j.eurpolymj.2019.05.014.
[63] B.K. Tarus, N. Fadel, A. Al-Oufy, M. El-Messiry, Investigation of mechanical properties of electrospun poly (vinyl chloride) polymer nanoengineered composite, J. Eng. Fibers Fabrics 15 (2020), 1558925020982569.
[64] M. Ago, J.E. Jakes, O.J. Rojas, Thermomechanical properties of lignin-based electrospun nanofibers and films reinforced with cellulose nanocrystals: a dynamic mechanical and nanoindentation study, ACS Appl. Mater. Interfaces 5 (22) (2013) 11768–11776, https://doi.org/10.1021/am403451w.
[65] V. Sessini, M.P. Arrieta, A. Fernández-Torres, L. Peponi, Humidity-activated shape memory effect on plasticized starch-based biomaterials, Carbohydr. Polym. 179 (2018) 93–99, https://doi.org/10.1016/j.carbpol.2017.09.070.
[66] A. Giannakas, M. Vlacha, C. Salmas, A. Leontiou, P. Katapodis, H. Stamatis, N. M. Barkoula, A. Ladavos, Preparation, characterization, mechanical, barrier and antimicrobial properties of chitosan/PVOH/clay nanocomposites, Carbohydr. Polym. 140 (2016) 408–415, https://doi.org/10.1016/j.carbpol.2015.12.072.
[67] S.Z. Hoseyni, S.M. Jafari, H.S. Tabarestani, M. Ghorbani, E. Assadpour, M. Sabaghi, Production and characterization of catechin-loaded electrospun nanofibers from Azivash gum-polyvinyl alcohol, Carbohydr. Polym. 235 (2020), 115979, https://doi.org/10.1016/j.carbpol.2020.115979.
[68] M. Ma, H.J. Di, H. Zhang, J.H. Yao, J. Dong, G.J. Yan, H.-Z. Qiao, J. Chen, Development of phospholipid vesicle-based permeation assay models capable of evaluating percutaneous penetration enhancing effect, Drug Dev. Ind. Pharm. 43 (12) (2017) 2055–2063, https://doi.org/10.1080/03639045.2017.1371730.
[69] J. Bonilla, E. Fortunati, L. Atarés, A. Chiralt, J.M. Kenny, Physical, structural and antimicrobial properties of poly vinyl alcohol–chitosan biodegradable films, Food Hydrocoll. (2014) 35463–35470, https://doi.org/10.1016/j.foodhyd.2013.07.002.
[70] S. Mandal, A.K. Dasmahapatra, Effect of aging on the microstructure and physical properties of Poly (vinyl alcohol) hydrogel, J. Polym. Res. 28 (7) (2021) 1–12, https://doi.org/10.1007/s10965-021-02624-9.
[71] L. Dai, C. Sun, D. Wang, Y. Gao, The interaction between zein and lecithin in ethanol-water solution and characterization of zein–lecithin composite colloidal nanoparticles, PLoSOne 11 (11) (2016) 0167172, https://doi.org/10.1371/journal.pone.0167172.
[72] T. Patel, Y. Ishiuji, G. Yosipovitch, Menthol: a refreshing look at this ancient compound, J. Am. Acad. Derm. 57 (5) (2007) 873–878, https://doi.org/10.1016/j.jaad.2007.04.008.
[73] G.P. Kamatou, I. Vermaak, A.M. Viljoen, B.M. Lawrence, Menthol: a simple monoterpene with remarkable biological properties, Phytochemistry 96 (2013) 15–25, https://doi.org/10.1016/j.phytochem.2013.08.005.
[74] L.T. Fox, M. Gerber, J.D. Plessis, J.H. Hamman, Transdermal drug deliveryenhancement by compounds of natural origin, Molecules 16 (2011) 10507–10540, https://doi.org/10.3390/molecules161210507.
[75] M.S. Kapoor, S. GuhaSarkar, R. Banerjee, Stratum corneum modulation by chemical enhancers and lipid nanostructures: implications for transdermal drug delivery, Ther. Del. 8 (8) (2017) 701–718, https://doi.org/10.4155/tde-2017-0045.
[76] J. Wang, F. Guo, M. Ma, M. Lei, F. Tan, N. Li, Nanovesicular system containing tretinoin for dermal targeting delivery and rosacea treatment: a comparison of hexosomes, glycerosomes, and ethosomes, RSC Adv. 4 (85) (2014) 45458–45466, https://doi.org/10.1039/C4RA08488H.
[77] M. Boncheva, F. Damien, V. Normand, Molecular organization of the lipid matrix in intact stratum corneum using ATR-FTIR spectroscopy, Biochim. Biophys. Acta (BBA) Biomem. 1778 (5) (2008) 1344–1355, https://doi.org/10.1016/j.bbamem.2008.01.022.
[78] A.I. Barbosa, S.A.C. Lima, I. Yousef, S. Reis, Evaluating the skin interactions and permeation of alginate/fucoidan hydrogels per se and associated with different essential oils, Pharmaceutics 15 (1) (2023) 190, https://doi.org/10.3390/pharmaceutics15010190.
[79] T. Caon, C.E.M. Campos, C.M.O. Simões, M.A.S. Silva, Novel perspectives in the tuberculosis treatment: administration of isoniazid through the skin, Int. J. Pharm. 494 (1) (2015) 463–470, https://doi.org/10.1016/j.ijpharm.2015.08.067.